JOURNAL OF QUATERNARY SCIENCE (2020) **35**(1-2) 93–101 ISSN 0267-8179. DOI: 10.1002/jqs.3176

JQS Journal of Quaternary Science QRA Quaternary Research Association

Dawson tephra, a widespread 29-ka marker bed, in a marine core from Patton Seamount off the Alaska Peninsula and its potential marine–terrestrial correlation

KAORI AOKI*
Tokyo Metropolitan University, Hachioji City, Tokyo, Japan

Received 2 March 2019; Revised 28 November 2019; Accepted 29 November 2019

ABSTRACT: A tephra layer with normal grading in the sub-bottom depth interval 119–122 cm in marine core SO202-27-6 was collected on Patton Seamount in the northeast North Pacific Ocean. Based on the geochemistry of volcanic glass shards determined by a wavelength dispersive electron probe micro-analyser and an X-ray fluorescence analyser, this layer is correlated to the Dawson tephra, a widespread late Pleistocene time marker tephra in Alaska and the Yukon. The age of the Dawson tephra in the core is 29.03 ± 0.178 ka (1 sigma) based on a published age model. The Dawson tephra is revealed to have been deposited in the transition from marine isotope stage 3 to 2, i.e. the last stage of Heinrich Stadial 3 derived from the ice-rafted debris signal. According to the correlation between Greenland (NGRIP ice core) and this core, the Dawson tephra occupies the record immediately before inter stadial 4 in the $\delta^{18}O$ stratigraphy of NGRIP. The Dawson tephra on Patton Seamount includes lithic fragments, which suggests that it was deposited not only by fall-out but also in part via another mechanism, such as icebergs from the Cordilleran ice sheet or seasonal sea ice. Copyright © 2019 John Wiley & Sons, Ltd.

KEYWORDS: Dawson tephra; Heinrich Stadial; late Pleistocene; marine sediment; MIS3/2.

Introduction

Quaternary pelagic sediments in the northeastern Pacific Ocean facing the Aleutian–Alaska volcanic zone yield many distal tephra layers. In the 1960s, the organisation presently known as the Lamont–Doherty Earth Observatory in the United States undertook research on pelagic sedimentary cores collected from the northern Pacific with *RV VEMA*, and Ninkovich *et al.* (1966) and Horn *et al.* (1969) reported the distribution of tephras.

Smith and Westgate (1968) succeeded in correlating widespread tephra beds at distal sites using the geochemistry of volcanic glass shards determined by microprobe for the first time. Later, from the 1970s to the 1980s, Quaternary tephrostratigraphy was diligently reconstructed with palaeoenvironmental studies in addition to geochemical analyses, and the field of tephrochronology developed with new dating methods. Then, in the 1990s, great progress in palaeoceanographic study in the northern Atlantic promoted tephra correlations in pelagic sediments, which were traced to anywhere in northern European countries (e.g. Lacasse *et al.*, 1995; Davies *et al.*, 2003; Wastegård, 2005). Additionally, in the northwestern Pacific Ocean, several late Quaternary tephras were correlated in marine sedimentary cores, and their eruptive ages and stratigraphic positions in the oxygen isotope stages of foraminiferal fossils were reported (Aoki and Arai, 2000; Aoki and Sakamoto, 2003; Aoki, 2008; Aoki *et al.*, 2008). The list of more recent papers on tephra correlations in marine sedimentary cores could continue.

Additionally, the knowledge of Quaternary volcanism and tephrostratigraphy in and around the Aleutian–Alaska Peninsula and Yukon region has been advancing rapidly (e.g. Westgate *et al.*, 1985; Westgate, 1989; Mangan *et al.*, 2003; Froese *et al.*, 2006; Jensen *et al.*, 2008; Feeley and Winer, 2009; Reyes *et al.*, 2010; Preece *et al.*, 2000, 2011; Jensen *et al.*, 2013; Turner *et al.*, 2013; Davies *et al.*, 2016; Jensen *et al.*, 2016). Such Quaternary tephrostratigraphy has contributed to reconstructing palaeoenvironmental changes during glacial and interglacial intervals in the Arctic. Furthermore, tephrostratigraphy serves as a useful and powerful tool linking on-land palaeoenvironmental studies to marine chronological studies in the North Pacific and its surrounding marginal seas, such as the Bering Sea. Here, the case of the Dawson tephra is presented, a widespread late Pleistocene tephra correlated in the northeastern North Pacific Ocean, including new information on its composition, eruptive age and stratigraphic position obtained from palaeoceanographic proxies in a sedimentary core.

Regional setting of the study area

Here, the geographic setting of the study area is briefly summarised (Fig. 1). The sedimentary box core SO202-27-6 (30 cm by 30 cm) was collected from Patton Seamount in the northeastern Pacific Ocean during the SO202-Innovative North Pacific Experiment (INOPEX) cruise in summer 2009 (Gersonde and SO202-INOPEX participants, 2010). The core was located on Patton Seamount at latitude 54°17.77′N and longitude 149°36.01′W at a depth of 2919 m. The surface circulation in the subarctic Pacific is the Subarctic Gyre, which is dominated by wind-driven cyclones (Maier *et al.*, 2015).

Quaternary volcanoes adjacent to the subarctic Pacific are found mainly in the Aleutian–Alaska volcanic zone, which spans 2500 km along the Aleutian arc front stretching to the Alaska Peninsula (Fig. 1). According to the Alaska Volcano Observatory (https://www.avo.alaska.edu/volcanoes/about.php), Alaska contains more than 130 volcanoes and volcanic fields that have been active within the last two million years

*Correspondence: K. Aoki, as above.
E-mail: aokikao@tmu.ac.jp

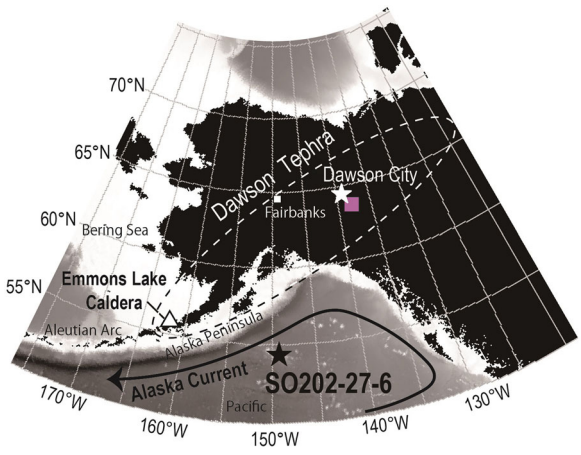

Figure 1. Location of coring sites in the study area and the distribution of the Dawson tephra (Froese *et al.*, 2002). Note: Map based on the GEBCO_2014 (Weatherall, *et al.*, 2015). The black star is the site of sedimentary core SO202-27-6 on Patton Seamount. The white star is the Dawson City. The pink square area is the Klondike area in Yukon, in which distal Dawson tephra was recognised for the first time. The white triangle is the Emmons Lake volcanic centre (ELVC; Mangan *et al.*, 2003). [Color figure can be viewed at wileyonlinelibrary.com].

(DGGS Staff *et al.*, 2008). Such Quaternary volcanoes have provided many tephras in and around large areas of Alaska and the Yukon (e.g. Jensen *et al.*, 2016). In particular, the Old Crow tephra (124 ± 10 ka; Westgate *et al.*, 1983; Preece *et al.*, 2011), Dawson tephra (ca. 30 ka; Froese *et al.*, 2002; Jensen *et al.*, 2016), and Aniakchak II (3572 ± 4 cal BP; Pearce *et al.*, 2017; Ponomareva *et al.*, 2018) are significant widespread tephras in this area.

Materials and methods

The sedimentary box core SO202-27-6 consists of pelagic ooze, and its sub-bottom depth is 2.92 m below the sea floor (Fig. 2). The colour of the sediment is brown on top and gradually changes to olive brown (Gersonde and SO202-INOPEX participants, 2010). The bottom 1 m of the core shows laminated dark grey and light yellow–grey zones, with a moderate transition. Dropstones are included throughout the core. Maier *et al.* (2018) reported the chronology and palaeoceanographic environment of core SO202-27-6 using multiple geochemical methods and model experiments. They adopted twelve ^{14}C dates, in which additional local reservoir ages of sinistral *Neogloboquadrina pachyderma* were applied in combination with fifteen other age control points, and constructed an age model through proxy correlations to the high-resolution Lake Suigetsu record and the NGRIP dust record. As a result, the bottom of the core was revealed to represent ca. 50 ka during MIS 3. This paper employs the age model of Maier *et al.* (2018).

Normal grading is recognised in the tephra layer at sub-bottom depths of 119–122 cm (Samples ID93 and ID94 in the cruise report which we henceforth refer to as the 119–122 cm tephra). The bottom of the layer shows a sharp contact with the lower ooze, and the upper boundary is unclear (Fig. 3(a)). Samples were washed with fresh water and decanted, dried naturally, and sieved by meshes with diameters of 250, 125 and 63 μm. Every tephra grain was observed under a binocular microscope. The tephra deposit consists of irregularly shaped and sized lithic and pumice fragments and well-sorted whitish grey ash-sized grains. Irregularly shaped and sized lithic grains are grey or black in colour, and their diameters are ~ 10 mm (Fig. 3(b) and (c)). The geochemical characteristics of the glass shards were determined, which are 125–250 μm in size, from the tephra layer sample ID93 and discuss its correlatives, age, and depositional palaeoenvironment.

The geochemistry of the constituent glass of the tephra was examined by two methods. The major element chemistry of volcanic glass shards in the 125–250 μm size fraction was determined using a wavelength dispersive electron probe micro-analyser (EPMA) JEOL JXA-8200 located at the Center for Advanced Marine Core Research, Kochi University. The

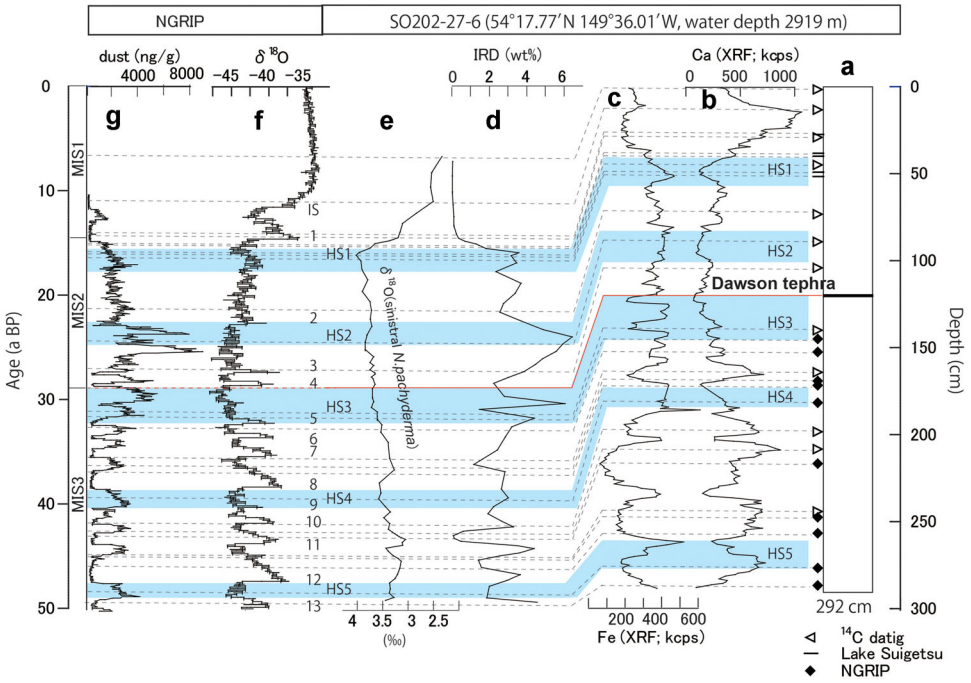

Figure 2. Proxy data from the sedimentary core SO202-27-6 and NGRIP. Notes: (a) Section of the sedimentary core SO202-27-6. (b) Calcium intensity based on XRF analysis. (c) Iron intensity based on XRF analysis. (d) IRD profile. (e) δ^{18}O data from sinistral *N. pachyderma*. (f) NGRIP δ^{18}O record. (g) NGRIP dust concentration. (a): quoted from Gersonde R. and SO202-INOPEX participants (2010). (b)–(e): quoted from Maier *et al.* (2018). (f): quoted from North Greenland Ice Core Project members (2004). (g): quoted from Ruth *et al.* (2007). [Color figure can be viewed at wileyonlinelibrary.com].

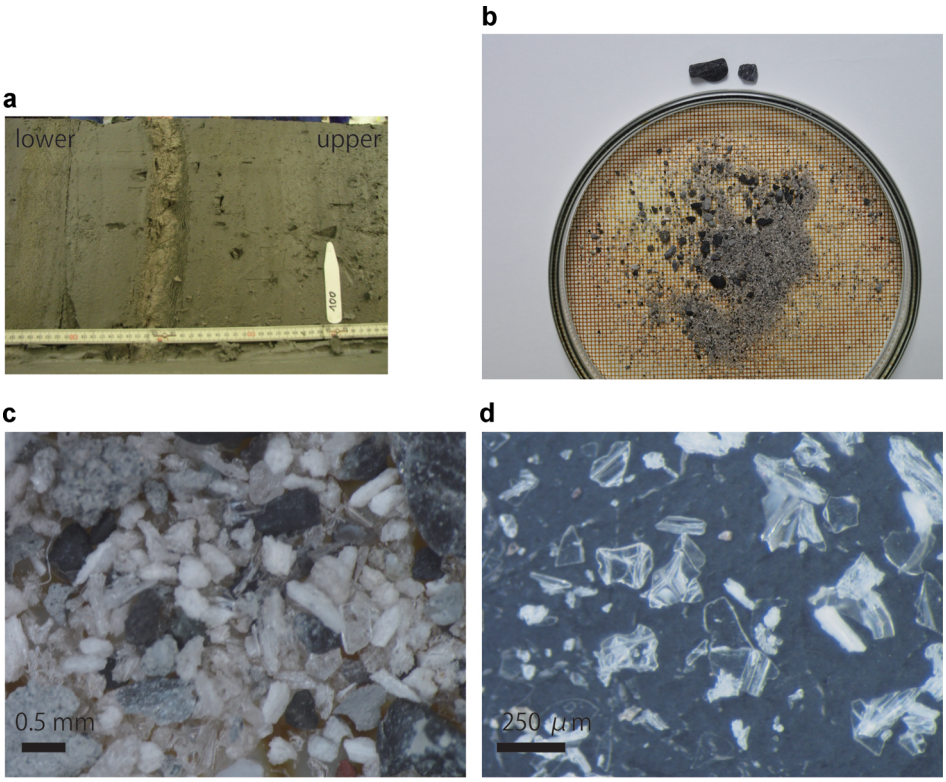

Figure 3. (a) Photograph of the tephra layer (119–122 cm) in the sedimentary core SO202-27-6. Note: The white point marks 100 cm. (b) Photograph of washed tephra samples (119–122 cm) in a dish with a 1 mm grid square. Note: Lithic fragments (~ 10 mm) are placed outside of the dish. (c) Photomicrograph of white feldspar and colourless glass shards more than 250 μm in size under the stereoscopic microscope. (d) Photomicrograph of grains, mainly glass, with diameters in the range of 125–250 μm under the stereoscopic microscope. [Color figure can be viewed at wileyonlinelibrary.com].

EPMA was operated at 15 kV using a 10 nA beam current and a 10 μm beam diameter to minimise the loss of Na and K (Froggatt, 1992). Na and K were always analysed before any other element. Peak counting times of 10 seconds were used. The weights of each element were calculated by the ZAF method using mineral standard samples (quartz, rutile, corundum, haematite, manganosite, wollastonite, periclase, albite and K-feldspar). Glass shards of the Aira-Tn (AT) tephra (Machida and Arai, 1976, 1992, 2003) and obsidian from Wada Touge were used to monitor the reproducibility of the data and stability of the instrument (Appendix 1).

Furthermore, the major and minor element compositions (SiO_2, TiO_2, Al_2O_3, FeO, MnO, MgO, CaO, Na_2O, K_2O, Ba, Co, Cr, Cu, Ga, Nb, Ni, Pb, Rb, Sr, Th, V, Y, Zn and Zr) of volcanic glass shards in the 125–250 μm size fraction were determined using an X-ray fluorescence analyser (XRF; Rigaku ZSX Primus II) located at Rissho University (Kawano, 2010). Before making the glass beads, the volcanic glass samples from the 125–250 μm size fraction were rinsed in very weak HCl diluted with water so that the hydrochloric acid concentrate was ≤1.0% by weight/volume to dissolve some contaminating calcareous microfossils. Next, the shards were rinsed in pure water again and dried naturally. The glass samples (2.67 g) were mixed with lithium tetraborate ($Li_2B_4O_7$) and the glass beads were prepared for quantitative analysis.

Results of glass shard analysis

Geochemical character of glass and its correlation

The major element compositions of volcanic glass shards determined by EPMA are shown in Table 1. Its character is very felsic (SiO_2 is 74.1 wt%, Al_2O_3 is 13.8 wt%, and Na_2O+K_2O is 8.35 wt%), and the mafic contents are not as high (FeO* is 2.00 wt%, and MgO is 0.21 wt%). The broad trend of major element compositions determined by XRF shown in Table 2 is similar to that of major element compositions by EPMA; however, the contents of Al_2O_3 (14.6 wt%), FeO* (3.52 wt%), CaO (2.50 wt%) and MgO (0.85 wt%) are higher, and SiO_2 (70.4 wt%) and K_2O (3.20 wt%) are lower than EPMA data because of contaminating minerals.

The new geochemical character of these volcanic glass shards is very similar to that of the Dawson tephra (ca. 30 ka; age from Davies *et al.*, 2016). The Dawson tephra was erupted from the Emmons Lake volcanic centre on the Alaska Peninsula during the late Pleistocene and is found in loess deposits from west-central Yukon (Mangan *et al.*, 2003, 2009). Mangan *et al.* (2003), Preece *et al.* (2011) and Jensen *et al.* (2016) showed geochemical data for volcanic glass shards in the Dawson tephra and its correlatives collected in Alaska and Yukon (Table 1 and Fig. 4). SC values (Borchardt *et al.*, 1972) calculated between the tephra layer (119–122 cm) and reference data are in the range of 0.92–0.96, except for sample 00s16ml in Mangan *et al.* (2003) (Table 1). FeO* in 00s16ml is slightly higher than in other upper parts of flow deposits and distal Dawson tephra data. This sample was collected from the basement of pumice flow deposits approximately 10 km northeast of the caldera, so its composition might reflect minor heterogeneity, although Mangan *et al.* (2003) did not discuss it.

The major element compositions of the 119–122 cm tephra determined by XRF are shown in Table 2 with the whole-rock data of pumice clasts by XRF (Mangan *et al.*, 2003). Generally, regarding the balance of compositions, they correlate with each other. However, FeO (3.52 wt%) and CaO (2.50 wt%) in this paper are slightly higher than FeO (2.79 wt%) and CaO (1.96 wt%) in Mangan *et al.* (2003). This difference is presumed to be the influence of the bulk sample contaminated by exiguous orthopyroxene and plagioclase.

The minor element compositions determined by XRF are shown in Table 3 with some elements from the minor element compositions of volcanic glass shards determined by solution inductively coupled plasma mass spectrometry (ICP-MS) in Mangan *et al.* (2003) and Preece *et al.* (2011). Comparable elements are Ba, Nb, Pb, Rb, Sr, Th, Y and Zr. Seven elements

Table 1. Glass shard major element compositions of the tephra layer (119-122 cm) in the sedimentary core SO202-27-6 and reference data for Dawson tephra correlatives determined by EPMA.

	SiO_2	TiO_2	Al_2O_3	FeO*	MnO	CaO	MgO	Na_2O	K_2O		Total	*n*	SC
This study, SO202-27-6, 119–122 cm													
ID93	74.1	0.25	13.8	2.00	0.06	1.22	0.21	4.43	3.92		97.3	24	
	0.3	0.0	0.1	0.1	0.0	0.1	0.0	0.1	0.1		1.1		
Dawson tephra (Mangan *et al*, 2003, Can. J. Earth Sci.)													
	SiO_2	TiO_2	Al_2O_3	FeO*	MnO	CaO	MgO	Na_2O	K_2O	P_2O_5	Total		
99slml	74.2	0.30	13.7	2.10	0.09	1.23	0.24	4.52	3.67	0.03	-	10	**0.92**
	0.4	0.1	0.1	0.2	0.1	0.0	0.0	0.3	0.1	0.0			
00s16m8	74.3	0.26	13.5	1.93	0.09	1.13	0.22	4.64	3.90	0.03	-	7	**0.94**
	0.6	0.1	0.3	0.1	0.0	0.1	0.1	0.3	0.6	0.0			
00s16ml	74.2	0.31	13.6	2.47	0.06	1.17	0.26	4.33	3.52	0.03	-	5	**0.90**
	0.9	0.1	0.2	0.3	0.1	0.0	0.1	0.5	0.1	0.0			
UT540	74.9	0.29	13.7	1.97	0.08	1.21	0.22	4.06	3.60	0.03	-	15	**0.93**
	0.9	0.1	0.1	0.1	0.1	0.1	0.0	0.1	0.9	0.0			
Dawson tephra (Jensen *et al.*, 2016, Qut. Sci. Rev.)													
	SiO_2	TiO_2	Al_2O_3	FeO*	MnO	CaO	MgO	Na_2O	K_2O	Cl	H_2Od		
UA1000	74.1	0.27	13.7	2.05	0.07	1.24	0.22	4.52	3.68	0.22	3.67	39	**1**
	0.3	0.0	0.2	0.1	0.0	0.1	0.0	0.2	0.1	0.0	2.3		
HH8	74.2	0.28	13.5	2.12	0.08	1.27	0.23	4.44	3.58	0.23	4.60	9	**0.9**
	0.3	0.1	0.2	0.2	0.0	0.1	0.1	0.4	0.1	0.0	2.2		
Dawson tephra (Preece *et al.*, 2011, Qut. Sci. Rev.)													
	SiO_2	TiO_2	Al_2O_3	FeO*	MnO	CaO	MgO	Na_2O	K_2O	Cl	H_2Od	n	
Dawson	74.2	0.27	13.7	2.05	0.07	1.26	0.21	4.43	3.64	0.21	2.15	329	**1**
tephra	0.3	0.1	0.2	0.1	0.0	0.1	0.0	0.2	0.1	0.0	1.6		

Instrument: JXA-8200, JEOL Co., Japan, located at the Center for Advanced Marine Core Research, Kochi University. Total iron is shown as FeO*. The results were recalculated to 100% on a volatile-free basis and presented as the mean and standard deviation for n particles of glass shards. Total** represents raw data (before normalization).

except Sr are approximately similar in composition to those in Mangan *et al.* (2003) and Preece *et al.* (2011). The content of Sr in this study is twice that of the pure glass samples in Mangan *et al.* (2003) and Preece *et al.* (2011). This result is consistent with the influence of orthopyroxene and plagioclase presumed from the major element composition because Sr often substitutes for Ca in minerals.

Chronology

Maier *et al.* (2018) presented an age model of the sedimentary core SO202-27-6 based on twelve ^{14}C dating ages and fifteen control points correlated to NGRIP data and Lake Suigetsu data. The stratigraphic position of the 119–122 cm tephra as correlative to the Dawson tephra is supported by the age model and bounding radiocarbon dates on foraminiferal fossils. Sample ID OS-87892 collected from a sub-bottom depth of 103.5 cm is 23 800 ± 110 a BP, so the age calibrated by Marine 13 (Reimer *et al.*, 2013) using local reservoir ages determined for nearby MD02-2489 (Sarnthein *et al.*, 2015) is 27 022 cal a BP. Sample ID OS-88043 collected from a sub-bottom depth of 139.5 cm is 28 300 ± 140 a BP, so the calibrated age is 31 303 cal a BP. Based on such dating, the 119–122 cm tephra as the Dawson tephra correlative in this sediment core is estimated to have been deposited at 29.03 ± 0.178 cal ka BP (1 sigma range). Furthermore, Maier *et al.* (2018) reported synchronous signals, such as Heinrich Stadials (HS) in the North Atlantic Ocean, between the signals of ice-rafted debris (IRD) and the freshwater discharge to the northeastern North Pacific from the Cordilleran ice sheet (CIS) based on multiple palaeoceanographic proxies from sediment core SO202-27-6. The Dawson tephra lies within the transition from MIS 3 to MIS 2 and the last stage of HS 3 derived from the IRD signal (Fig. 2). Furthermore, the correlations between NGRIP and this core indicate that this tephra formed just before interstadial (IS) 4 of the $\delta^{18}O$ stratigraphy in the NGRIP data (IS 4; Fig. 2).

Glass morphology and mineral assemblages

Well-sorted ash-sized grains in the 119–122 cm tephra include the maximum diameter of white pumice grains, which is approximately 2 mm, and volcanic glass shards; the latter are parts of the junctions of bubbles over 250 μm and are mainly clear, although some of them clearly tend slightly to brown. The grain size of 125–250 μm is very glassy and consists of white to clear sponge-type and bubble wall-type glass shards (Fig. 3(d)). On the other

Table 2. Glass shard major element compositions of the tephra layer (119-122 cm) in the sedimentary core SO202-27-6 and reference data for Dawson tephra correlatives determined by XRF.

	SiO_2	TiO_2	Al_2O_3	FeO*	MnO	MgO	CaO	Na_2O	K_2O	P_2O_5	*n*
SO202-27-6, 119–122 cm(63–125 μm glass shards)											
ID93	70.4	0.45	14.6	3.52	0.09	0.85	2.50	4.31	3.20	0.08	1
Dawson tephra (Mangan *et al.*, 2003, Can. J. Earth Sci.)											
Pumice clasts	71.6	0.34	14.6	2.79	0.08	0.64	1.96	4.47	3.47	0.07	10
(whole rock XRF)	1.4	0.1	0.5	0.5	0.0	0.2	0.5	0.1	0.2	0.0	

Instrument: ZSX Primus II, Rigaku, Japan, located at Rissho University.

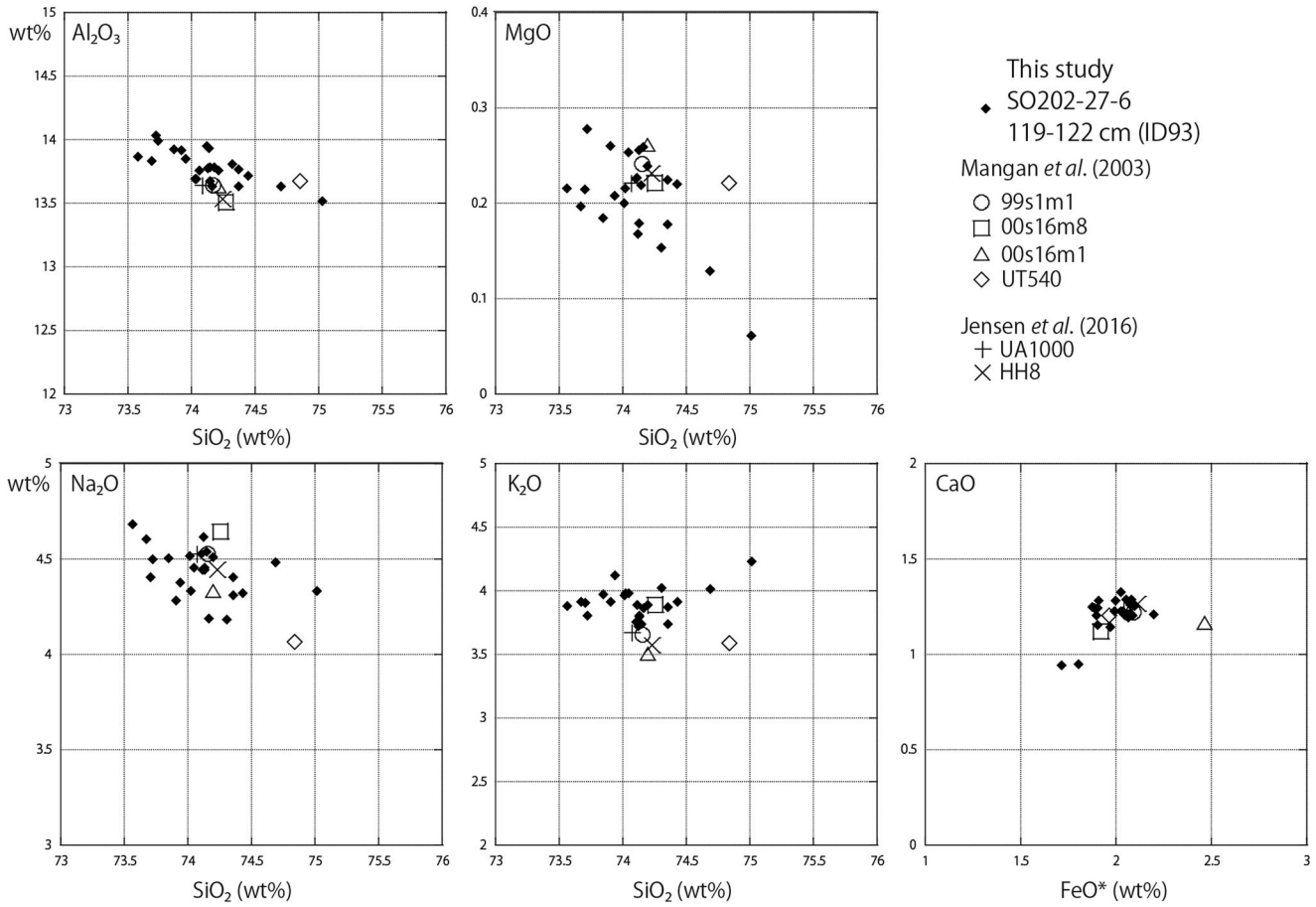

Figure 4. Diagrams of normalised SiO_2 versus Al_2O_3, MgO, Na_2O and K_2O and FeO* versus CaO contents in volcanic glass shards from the tephra layer (119–122 cm) and reference data for Dawson tephra correlatives determined by EPMA. Note: Data are shown in Table 1.

hand, small amounts of minerals are found in ash-sized grains. Under the binocular microscope, a few orthopyroxene and plagioclase grains with sizes of 63–250 μm are observed. Such a mineral assemblage is coincident with that of the Dawson tephra in the Yukon region (Naeser *et al.*, 1982). This fact suggests that they are derived from fall-out deposits at the distal site.

Discussion

The Dawson tephra is one of the distal tephra beds noted in the late Cenozoic deposits of the Klondike area in Yukon (Naeser *et al.*, 1982). Naeser *et al.* (1982) reported that it consists mainly of very fine bubble wall-type volcanic glass shards with a median diameter of 5.3 phi and that

Table 3. Glass shard trace element compositions of the tephra layer (119-122 cm) in the sedimentary core SO202-27-6 determined by XRF and reference data for Dawson tephra correlatives determined by solution ICP-MS.

SO202-27-6 119–122 cm this study		Dawson tephra (Mangan *et al*, 2003)					Dawson tephra (Preece *et al.*, 2011)	
XRF analysis	ID93	*solution ICP-MS*	UT540	99slml	00s16m8	00s16ml	*solution ICP-MS average of 9 samples*	
Ba	**810**	Ba	897	884	874	895	920	(52)
Co	10							
Cr	10							
Cu	20							
Ga	20							
Nb	**10**	Nb	7.77	7.82	7.90	8.13	7.31	(1.15)
Ni	10							
Pb	**20**	Pb	18.6	17.7	17.7	21.0		
Rb	**80**	Rb	83.3	82.7	85.3	90.3	85	(9)
Sr	**160**	Sr	75.7	93.9	94.5	88.8	73	(7)
Th	**10**	Th	8.66	8.43	8.62	8.95	7.5	(0.7)
V	40							
Y	**40**	Y	43.7	44.0	44.8	49.3	39.6	(2.2)
Zn	60							
Zr	**280**	Zr	190	194	195	298	299	(29)

Note: For comparison, excerpt trace element compositions overlapping the XRF data in this study are taken from Mangan *et al.* (2003) and Preece *et al.* (2011). Standard deviations in parentheses.

orthopyroxene is observed among the heavy minerals. Westgate *et al.* (2000) estimated that its thickness in west-central Yukon is in the range of 15–30 cm. Preece *et al.* (1999) and Westgate *et al.* (2000) indicated that the Dawson tephra in Yukon is a Type 1 tephra bed derived from a volcano in the Aleutian Arc–Alaska Peninsula region based on geochemistry, including the rare earth element profiles of volcanic glass shards. Later, Mangan *et al.* (2003) revealed that the source of the Dawson tephra was the Emmons Lake caldera (55° 20′ 27.24″ N, 162° 4′ 21.36″ W) in the Alaska Peninsula (Fig. 1). The Emmons Lake caldera, 19 km by 12 km, is nested in multiple volcanic structures, including stratovolcanoes and overlapping vents (Miller and Smith, 1987). Collectively, they are called the Emmons Lake volcanic centre (ELVC) on the southwestern end of the Alaska Peninsula. The ELVC experienced repeated silicic caldera-forming eruptions at least four or five times (Mangan *et al.*, 2009). The last major one was C2, which is correlated with the Dawson tephra (Mangan *et al.*, 2003). After the C2 event, andesitic and basaltic magma eruptions have occurred in the ELVC; during the last 200 years, more than 40 eruptive events have occurred, such as the 2016 eruption of the Pavlof volcano. The C2 event as the correlative of the Dawson tephra consists of pyroclastic flow deposits associated with the caldera-forming eruption. The ignimbrite extended in all directions from the caldera and reached the Bering Sea and North Pacific Ocean coastlines, covering a minimum area of 2500 km^2. The Klondike locality of the Dawson tephra in Yukon is located approximately 1700 km northeast of the ELVC.

Further, Begét *et al.* (2005) reported in an abstract the discovery of the Dawson tephra in Ocean Drilling Program (ODP) Leg 145, core 887B, collected from Patton Seamount near the site of SO202-27-6. Cao *et al.* (1995) reported the major element compositions of volcanic glass shards in ODP Leg 145 core 887 A. Data for five volcanic glass shards in sample 1H-2 from 36–37 cm (sub-bottom depth is 1.5 mbsf) resemble the geochemistry of the Dawson tephra (Table 4). Additionally, thin deposits of the Dawson tephra are present near Fairbanks, Alaska (Begét *et al.*, 2005; Jensen *et al.*, 2016). Based on the results of this paper and the above information, the distribution map of the Dawson tephra should be revised from the conventional dispersed area map (Froese *et al.*, 2002). In future work, more marine sediment cores in the Gulf of Alaska and the eastern North Pacific will be needed.

Radiocarbon dating of the Dawson tephra in the Klondike area and the C2 event around the ELVC has been reported several times and range from approximately 27 000 to 31 000 cal a BP (Table 5: Froese *et al.*, 2002, 2006; Mangan *et al.*, 2003; Demuro *et al.*, 2008; Davies *et al.*, 2016). Demuro *et al.* (2008) reported additional ^{14}C ages from dating in addition to the calibrated ages from ^{14}C dating quoted in previous studies and estimated the depositional age of the Dawson tephra as ranging from 30 433 cal a BP to 30 014 cal a BP using the Bayesian model. The present result that the Dawson tephra correlative in this core was deposited at 29.03 ± 0.178 cal ka BP is close to the previously calibrated ^{14}C dating results on land. Demuro *et al.* (2008) reported additional ^{14}C dates from the Klondike and, using Bayesian methods, estimated an age of 30 430 to 30 015 (rounded to the nearest 5 years) cal a BP. Davies *et al.* (2016), using a Bayesian Tau_Boundary model, combined the ^{14}C, optically stimulated luminescence and fission-track dates associated with the Dawson tephra to give an age estimate of 29 055 to 29 470 cal a BP for the eruption. This age agrees with the ages suggested by Froese *et al.* (2006) and is slightly younger than the estimate of Demuro *et al.* (2008) but consistent with the marine ages presented in this paper. Given these age constraints, the Dawson tephra correlation in this core deposited at 29.03 ± 0.178 cal ka BP is consistent with the terrestrial record.

Table 5. Eruptive age of the Dawson tephra on land determined by radiocarbon dating.

^{14}C age (a BP)	Eruptive age (cal a BP)	Reference
24,000	ca. 27 000	Froese *et al.* (2002)
27,110	ca. 31 000	Mangan *et al.* (2003)
25,300	-	Froese *et al.* (2006)
25 420–25290	30 433–30 032	Demuro *et al.* (2008)
23520–25510	29055–29470	Davies *et al.* (2016)

Dispersed Dawson tephra has been discovered south of eastern Beringia (Fig. 1). The palaeoenvironmental conditions when it erupted and settled were as follows. All occurrences of the Dawson tephra are reported from the unglaciated Klondike area of west-central Yukon (Westgate *et al.*, 2000). At this time, a steppe-tundra ecosystem has been estimated to have covered the Klondike area, according to the analysis of pollen and microfossils (Zazula *et al.*, 2003, 2005, 2006; Froese *et al.*, 2006; Turner *et al.*, 2013). Jensen *et al.* (2016) noted that the highest profile of magnetic susceptibility above the Dawson tephra for the Alaskan loess in the Klondike area would be correlated to MIS 2. The palaeoenvironment reconstructed by the above studies when the Dawson tephra was deposited is summarised as follows: the Dawson tephra erupted at the transition from MIS 3 to MIS 2 (McConnell glaciation) under dry climate conditions, with a steppe-tundra ecosystem in the Klondike area. In this study, the stratigraphic position of the Dawson tephra is revealed to exactly record the transition of MIS 3/2 in marine sediment. Furthermore, using the age model correlated to NGRIP by Maier *et al.*

Table 4. Glass shard major element compositions of a tephra layer that might be correlated to the Dawson tephra from Cao *et al.* (1995).

Cao et al.(1995), ODP leg145, Hole887A, 1H-2, 36–37 cm (subbottm depth; 1.5mbsf)									
SiO_2	TiO_2	Al_2O_3	FeO*	MnO	MgO	CaO	Na_2O	K_2O	Total
75.0	0.2	13.6	1.9	-	-	1.2	4.5	3.6	98.3
75.0	0.2	13.7	2.0	-	-	1.2	4.4	3.6	104.2
75.0	0.2	13.8	2.2	-	-	1.2	3.7	3.4	99.2
75.7	0.1	13.4	2.1	-	-	1.1	4.2	3.5	100.1
75.3	0.1	13.6	2.0	-	-	1.2	4.3	3.6	100.6

Note: Data for five volcanic glass shards in sample 1H-2 at 36-37 cm (sub-bottom depth is 1.5 mbsf) are shown in Cao *et al.* (1995).

(2018), the Dawson tephra was present in the last stage of HS 3 (Fig. 2) in the northeastern North Pacific, which is found to be linked to HS in the North Atlantic Ocean, and below IS 4 of the NGRIP age model. Using the Dawson tephra as a tie point between the NGRIP age model and those reconstructed by other palaeoenvironmental proxies yields very valuable information to research the timing of the growth and collapse of the CIS and the linkage of global climate change and the North Pacific Ocean and to hunt for the Dawson tephra in ice cores from Greenland, such as the NGRIP core. Dispersed Dawson tephra is present south of eastern Beringia in the North Pacific Ocean on the basis of major element geochemistry, independent age control and the palaeoenvironmental setting. The Dawson tephra from the unglaciated Yukon area is found at the MIS 3 to 2 transition when a steppe-tundra ecosystem characterised the Klondike region (Zazula *et al.*, 2003, 2005, 2006; Froese *et al.* 2006). Similarly, in the Fairbanks area of Alaska, Jensen *et al.* (2016) studied the magnetic susceptibility of loess and demonstrated that the Dawson tephra was deposited as the wind intensity and colder climate conditions of MIS 2 developed following the warmer climate of MIS 3. In this study, the stratigraphic position of the Dawson tephra in the North Pacific marine records also indicates its deposition at the MIS 3/2 transition. Further, using the age model correlated with the NGRIP ice core record by Maier *et al.* (2018), the Dawson tephra was deposited in the final stage of HS 3 (Fig. 2) in the northeastern North Pacific. This marine–terrestrial correlation is interesting because it suggests that there is potential for using the Dawson tephra as an isochron between the marine–terrestrial and ice core records from the North Pacific through Greenland. What remains now is careful inspection of the NGRIP core or similar Greenland records to identify and confirm these correlations.

On the basis of the discovery and depositional age of the Dawson tephra in this study, one more problem to consider is its transport mechanism. The distance between the core site and the ELVC is 809 km. This layer shows normal grading, so the materials probably sank once. However, the layer includes volcanic ash containing a white pumice grain with a maximum diameter of approximately 2 mm, associated with some grey and black lithic fragments with diameters of ~10 mm (Fig. 3(b) and (c)). Therefore, it is hard to regard this layer as the only fall-out deposit around the core site. The fact that the Dawson tephra was present during the last stage of HS 3 (Maier *et al.*, 2018) suggests that it could have been transported by icebergs from the CIS. Hendy and Cosma (2008) presented potential IRD from the CIS during HSs in a sediment core off Vancouver Island. The Dawson tephra could have been transported as such IRD. Furthermore, Froese *et al.* (2006) noted that the Dawson tephra was deposited in the Klondike area when surface icing was active; thus, it erupted in the winter to spring. At this point, it is also possible to think that seasonal sea ice around the Alaska Peninsula might have transported the Dawson tephra. Modern seasonal sea ice in this area mainly expands into the Bering Sea, and some sea ice leaks into the North Pacific Ocean between islands of the Aleutian Island arc during the peak season (Fetterer *et al.*, 2017). Such sea ice has not recently reached the study area. However, its path is unknown during glacial periods. According to Ponomareva *et al.* (2018), a sediment core collected from the Chukchi Sea within the Arctic Circle contains many cryptic volcanic glass shards correlated to tephras provided from the volcanoes in the Aleutian–Alaska Peninsula region, such as the Dawson tephra, which might have experienced secondary transport. Furthermore, tephra deposits associated with IRD have been reported in previous research; for example, Ash Zone II in the North Atlantic Ocean (Austin *et al.*, 2004), numerous tephra deposits from Iceland and Jan Mayen in the Norwegian Sea (Brendryen *et al.*, 2010) and many of the southern Pacific tephra zones (Shane and Froggatt, 1992). Lowe (2011) suggested that anomalous grain size patterns may also indicate reworking and present one potential difficulty in tephra mapping. Thus, in high-latitude areas, it is possible that the transport mechanism of tephra is complex and may involve the influence of icebergs and/or sea ice. Perhaps the distribution map of the Dawson tephra, especially in the Pacific area, would connect to reveal a snapshot of the extent of icebergs or sea ice in the last stage of HS 3.

Conclusion

A tephra layer is recognised to show normal grading in the sub-bottom depth interval from 119–122 cm in the sedimentary core SO202-27-6 collected on Patton Seamount in the northeastern North Pacific Ocean. Based on the geochemistry and morphology of volcanic glass shards and on the mineral assemblage, it is correlated to the Dawson tephra, one of the widespread time marker tephras in Alaska and the Yukon area during the late Pleistocene, which was sourced from the ELVC on the southwestern Alaska Peninsula. The depositional age of the Dawson tephra correlative is obtained as 29.03 ± 0.178 cal ka BP from the age model of the sedimentary core (Maier *et al.*, 2018). Additionally, it is revealed that the Dawson tephra represents the transition from MIS 3 to MIS 2, i.e. the last stage of HS 3 derived from the IRD signal to be exact (Fig. 2). According to the correlation between NGRIP and this core, the tephra could be present just before IS 4 in the $\delta^{18}O$ stratigraphy of the NGRIP data. Such information encourages connecting the palaeoenvironmental changes around the CIS to global climate changes using the Dawson tephra as a tie point in the age model.

The distribution of the Dawson tephra in the North Pacific Ocean should be reviewed. The Dawson tephra correlative on Patton Seamount includes lithic fragments, so it likely reached this position not only by the fall-out process from the air but also another transport mechanism, such as icebergs collapsing from the CIS or seasonal sea ice. The distribution isopachs of the Dawson tephra in the ocean would be warped by the influence of icebergs and/or seasonal sea ice as distinctive mechanisms within the Arctic Circle.

Acknowledgements. This work was largely part of the Innovative North Pacific Experiment (INOPEX), funded by the German Ministry of Education and Science (Bundesministerium für Bildung und Forschung). I thank Dr. Rainer Gersonde, chief scientist of INOPEX, for inviting me to INOPEX and for his scientific advice. I have been using an EPMA since 2011 at one of the facilities in the Center for Advanced Marine Core Research of Kochi University, which is a nationwide joint-use system designed for scientists and students in Japan and is organized by the Ministry of Education, Culture, Sports, Science and Technology (MEXT). I am especially grateful for support by Prof. Y. Yamamoto and Dr. T. Matsuzaki, Kochi University. I thank the captain of the *R/V* Sonne, L. Mallon, as well as the crew members and the scientists on board for their remarkable work.

Supporting information

Additional supporting information may be found in the online version of this article at the publisher's web-site.

Supplementary data for individual data of volcanic glass shards of the tephra layer (119–122 cm) in the sedimentary core SO202-27-6 and the AT tephra as the standard data.

References

Aoki K. 2008. Revised age and distribution of ca. 87 ka Aso-4 tephra based on new evidence from the northwest Pacific Ocean. *Quaternary International* **178**: 100–118.

Aoki K, Arai F. 2000. Late Quaternary tephrostratigraphy of marine core KH94-3, LM-8 off Sanriku, Japan. *The Quaternary Research (Japan Association for Quaternary Research)* **39**: 107–120. (In Japanese with English abstract).

Aoki K, Sakamoto T 2003. Late Quaternary tephrostratigraphy of marine sediments from the Japan Trench forearc, Holes 1150 A and 1151 C. In *Proceedings of the Ocean Drilling Program, Scientific Results*, Suyehiro K, Sacks IS, Acton GD, Oda M (eds). p. 186.

Aoki K, Irino T, Oba T. 2008. Middle-late Pleistocene tephrostratigraphy of the sediment core MD01-2421 collected off the Kashima coast, Japan. *The Quaternary Research (Japan Association for Quaternary Research)* **47**: 391–407. (In Japanese with English abstract).

Austin WEN, Wilson LJ, Hunt JB. 2004. The age and chronostratigraphical significance of North Atlantic ash zone II. *Journal of Quaternary Science* **19**: 137–146.

Begét JE, Pedersen TF, Muhs D 2005. Terrestrial-marine correlation of the Dawson tephra. In *Proceedings of the International Field Conference and Workshop on Tephrochronology and Volcanism. Institute of Geological and Nuclear Sciences* , Alloway BV, *et al.* (eds). Lower Hutt, New Zealand: 58.

Borchardt GA, Aruscavage PJ, Millard HT Jr. 1972. Correlation of the Bishop Ash, a Pleistocene marker bed, using instrumental neutron activation analysis. *Journal of Sedimentary Petrology* **42**: 301–306.

Brendryen J, Haflidason H, Sejrup HP. 2010. Norwegian Sea tephrostratigraphy of marine isotope stages 4 and 5: prospects and problems for tephrochronology in the North Atlantic region. *Quaternary Science Reviews* **29**: 847–864.

Cao LQ, Arculus RJ, McKelvey BC 1995. Data report: geochemistry of volcanic ashes recovered from Hole 887 A. In *Proceedings of the Ocean Drilling Program, Scientifc Results, vol. 145*, Rea DK, Basov IA, Scholl DW, *et al.* (eds). Ocean Drilling Program: College Station, TX; 661–670.

Davies LJ, Jensen BJL, Froese DG, *et al.* 2016. Late Pleistocene and Holocene tephrostratigraphy of interior Alaska and Yukon: Key beds and chronologies over the past 30,000 years. *Quaternary Science Reviews* **146**: 28–53.

Davies SM, Wastegård S, Wohlfarth B. 2003. Extending the limits the Borrobol Tephra to Scandinavia and detection of new early Holocene tephras. *Quaternary Resarch* **59**: 345–352.

Demuro M, Roberts RG, Froese DG, *et al.* 2008. Optically stimulated luminescence dating of single and multiple grains of quartz from perennially frozen loess in western Yukon Territory, Canada: Comparison with radiocarbon chronologies for the late Pleistocene Dawson tephra. *Quaternary Geochronology* **3**: 346–364.

DGGS Staff, Nye CJ, Schaefer JR 2008. Alaska GeoSurvey News – The Alaska Volcano Observatory – 20 years of volcano research, monitoring, and eruption response. Alaska Division of Geological & Geophysical Surveys Newsletter 2008-1: 14 p. https://doi.org/10.14509/16061

Feeley TC, Winer GS. 2009. Volcanic hazards and potential risks on St. Paul Island, Pribilof Islands, Bering Sea, Alaska. *Journal of Volcanology and Geothermal Research* **182**: 57–66.

Fetterer F, Knowles K, Meier W, *et al.* 2017. *updated daily. Sea Ice Index, Version 3. [Indicate subset used].* NSIDC: National Snow and Ice Data Center: Boulder, Colorado USA. https://doi.org/10.7265/N5K072F8, [Date Accessed: 30 January 2019].

Froese DG, Westgate JA, Preece SJ, *et al.* 2002. Age and significance of the Late Pleistocene Dawson tephra in eastern Beringia. *Quaternary Science Reviews* **21**: 2137–2142.

Froese DG, Zazula GD, Reyes AV. 2006. Seasonality of the late Pleistocene Dawson tephra and exceptional preservation of a buried riparian surface in central Yukon Territory, Canada. *Quaternary Science Reviews* **25**: 1542–1551.

Froggatt PC. 1992. Standardization of the chemical analysis of tephra deposits. Report of the ICCT working group. *Quaternary International* **13/14**: 93–96.

Gersonde R, SO202-INOPEX participants. 2010. Cruise report of the SO202-INOPEX cruise. 181 pp.

Hendy IL, Cosma T. 2008. Vulnerability of the Cordilleran Ice Sheet to iceberg calving during late Quaternary rapid climate change events. *Paleocenography* **23**: PA2101, https://doi.org/10.1029/2008PA001606

Horn DR, Delach MN, Horn BM. 1969. Distribution of volcanic ash layers and turbidites in the north Pacific. *Geological Society of America Bulletin* **80**: 1715–1724.

Imai N, Terashima S, Itoh S, *et al.* 1995. 1994 Compilation of analytical data for minor and trace elements in seventeen gsj geochemical reference samples, "igneous rock series". *Geostandards Newsletter* **19**: 135–213.

Jensen BJL, Evans ME, Froese DG, *et al.* 2016. 150,000 years of loess accumulation in central Alaska. *Quaternary Science Reviews* **135**: 1–23.

Jensen BJL, Froese DG, Preece SJ, *et al.* 2008. An extensive middle to late Pleistocene tephrochronologic record from east-central Alaska. *Quaternary Science Reviews* **27**(3-4): 411–427.

Jensen BJL, Reyes AV, Froese DG, *et al.* 2013. The palisades is a key reference site for the middle pleistocene of eastern beringia: New evidence from paleomagnetics and regional tephrostratigraphy. *Quaternary Science Reviews* **63**: 91–108.

Kawano Y. 2010. Quantitative chemical analyses of silicate minerals using a scanning electron microscope with energy dispersive X ray detector. *Bulletin of geo-environmental science* **12**: 85–97. (In Japanese).

Lacasse C, Sigurdsson H, Johannesson H, *et al.* 1995. Source of Ash Zone 1 in the North Atlantic. *Bulletin of Volcanology* **57**: 18–32.

Lowe DJ. 2011. Tephrochronology and its application: A review. *Quaternary Geochronology* **6**: 107–153.

Machida H, Arai F. 1976. Kouiki ni bunpu suru Kazanbai- Aira Tn kazanbai no hakkenn to sono igi (Discovery of widespread Aira Tn tephra). *Kagaku* **46**: 339–347. (In Japanese).

Machida H, Arai F. 1992. *Atlas of tephra in and around Japan*. Tokyo University Press: Tokyo. (In Japanese).

Machida H, Arai F. 2003. *Atlas of tephra in and around Japan*. Tokyo University Press: Tokyo. (In Japanese).

Maier E, Méheust M, Abelmann A, *et al.* 2015. Deglacial subarctic Pacific surface water hydrography and nutrient dynamics and links to North Atlantic climate variability and atmospheric CO_2. *Paleoceanography* **30**: 949–968, https://doi.org/10.1002/2014PA002763

Maier E, Zhang X, Abelmann A, *et al.* 2018. North Pacific freshwater events linked to changes in glacial ocean circulation. *Nature* **559**: 241–245.

Mangan MT, Waythomas CF, Miller TP, *et al.* 2003. Emmons lake volcanic center, Alaska Peninsula: source of the Late Wisconsin Dawson tephra, Yukon territory, Canada. *Canadian Journal of Earth Sciences* **40**: 925–936.

Mangan M, Miller T, Waythomas C, *et al.* 2009. Diverse lavas from closely spaced volcanoes drawing from a common parent: Emmons Lake Volcanic Center, eastern Aluetian Arc. *Earth and Planetary Science Letters* **287**: 363–372.

Miller TP, Smith RL. 1987. Late Quaternary caldera-forming eruptions in the eastern Aleutian arc, Alaska. *Geology* **15**: 434–438

Naeser ND, Westgate JA, Hughes OL, *et al.* 1982. Fission track ages of late Cenozoic distal tephra beds in the Yukon and Alaska. *Canadian Journal of Earth Sciences* **19**: 2167–2178.

Ninkovich D, Opdyke N, Heezen BC, *et al.* 1966. Paleomagnetic stratigraphy, rates of deposition and tephrochronology in north pacific deep-sea sediments. *Earth and Planetary Science Letters* **1**: 476–492.

North Greenland Ice Core Project members. 2004. High-resolution record of Northern Hemisphere climate extending into the last interglacial period. *Nature* **431**: 147–151.

Turner D, Ward BC, Bond JD, *et al.* 2013. Middle to Late Pleistocene ice extents, tephrochronology and paleoenvironments of the White River area, southwest Yukon. *Quaternary Science Reviews* **75**: 59–77, https://doi.org/10.1016/j.quascirev.2013.05.011

Pearce C, Varhelyi A, Wastegård S, *et al.* 2017. The 3.6 ka Aniakchak tephra in the Arctic Ocean: a constraint on the Holocene radiocarbon reservoir age in the Chukchi Sea. *Climate of the Past* **13**: 303–316, https://doi.org/10.5194/cp-2016-112

Preece SJ, Westgate JA, Stemper BA, *et al.* 1999. Tephrochronology of late Cenozoic loess at Fairbanks, central Alaska. *Geological Society of America Bulletin* **111**: 71–90.

Preece SJ, Westgate JA, Alloway B, *et al.* 2000. Characterization, identity, distribution, and source of late Cenozoic tephra beds in the Klondike District of the Yukon, Canada. *Canadian Journal of Earth Sciences* **37**: 983–996.

Preece SJ, Pearce NJG, Westgate JA, *et al.* 2011. Old Crow tephra across eastern Beringia: a single cataclysmic eruption at the close of Marine Isotope stage 6. *Quaternary Science Reviews* **30**: 2069–2090, https://doi.org/10.1016/j.quascirev.2010.04.020

Ponomareva V, Polyak L, Portnyagin M, *et al.* 2018. Holocene tephra from the Chukchi-Alaskan margin, Arctic Ocean: Implications for sediment chronostratigraphy and volcanic history. *Quaternary Geochronology* **45**: 85–97.

Reimer PJ, Bard E, Bayliss A, *et al.* 2013. INTCAL13 and MARINE13 radiocarbon age calibration curves 0-50,000 years cal BP. *Radiocarbon* **55**: 1869–1887.

Reyes AV, Jensen BJL, Zazula GD, *et al.* 2010. A late-Middle Pleistocene (Marine Isotope Stage 6) vegetated surface buried by Old Crow tephra at the Palisades interior Alaska. *Quaternary Science Reviews* **29**: 801–811.

Ruth U, Bigler M, Röthlisberger R, *et al.* 2007. Ice core evidence for a very tight link between North Atlantic and east Asian glacial climate. *Geophysical Research Letters* **34**: L03706.

Sarnthein M, Balmer S, Grootes PM, *et al.* 2015. Planktic and benthic ^{14}C reservoir ages for three ocean basins calibrated by a suite of ^{14}C plateaus in the glacial-to-deglacial Suigetsu atmospheric ^{14}C record. *Radiocarbon* **57**: 129–151.

Shane PAR, Froggatt PC. 1992. Composition of widespread volcanic glass in deepsea sediments of the southern Pacific Ocean: an Antarctic source inferred. *Bulletin of Volcanology* **54**: 595–601.

Smith DGW, Westgate JA. 1968. Electron probe technique for characterizing pyroclastic deposits. *Earth and Planetary Science Letters* **5**: 313–319.

Wastegård S. 2005. Late Quaternary tephrochronology of Sweden: a review. *Quaternary International* **130**: 49–62.

Weatherall P, Marks KM, Jakobsson M, *et al.* 2015. A new digital bathymetric model of the world's oceans. *Earth and Space Science* **2**: 331–345, https://doi.org/10.1002/2015EA000107

Westgate JA, Hamilton TD, Gorton MP. 1983. Old Crow tephra: a new late Pleistocene stratigraphic marker across north-central Alaska and western Yukon Territory. *Quaternary Research* **19**: 38–54.

Westgate JA. 1989. Isothermal plateau fission-track ages of hydrated glass shards from silicic tephra beds. *Earth and Planetary Science Letters* **98**: 226–234.

Westgate JA, Walter RC, Pearce GW, *et al.* 1985. Distribution, stratigraphy, petrochemistry and palaeomagnetism of the late Pleistocene Old Crow tephra in Alaska and the Yukon. *Canadian Journal of Earth Sciences* **22**: 893–906.

Westgate JA, Preece SJ, Kotler E, *et al.* 2000. Dawson tephra: a prominent stratigraphic marker of late Wisconsin age in west-central Yukon. *Canadian Journal of Earth Sciences* **37**: 621–627.

Zazula GD, Froese DG, Schweger CE, *et al.* 2003. Ice age steppe vegetation in east Beringia. *Nature* **423**: 603.

Zazula GD, Froese DG, Westgate JA, *et al.* 2005. Paleoecology of Beringian ''packrat'' middens from central Yukon Territory, Canada. *Quaternary Research* **63**: 189–198.

Zazula GD, Schweger CE, Beaudoin AB, *et al.* 2006. Macrofossil and pollen evidence for full-glacial steppe within an ecological mosaic along the Bluefish River, eastern Beringia. *Quaternary International* **142–143**: 2–16.

Appendix: Glass shard major element compositions of Aira-Tn (AT) tephra and of two obsidian samples

	SiO_2	TiO_2	Al_2O_3	FeO*	MnO	CaO	MgO	Na_2O	K_2O	Total	*n*
first analyses											
RIS1	76.9	0.04	12.9	0.66	0.09	0.49	0.02	4.01	4.92	98.5	10
	0.2	0.0	0.2	0.1	0.0	0.0	0.0	0.1	0.1	0.4	
AT	77.5	0.11	12.6	1.25	0.06	1.07	0.12	3.73	3.55	94.9	10
	0.2	0.0	0.2	0.1	0.0	0.0	0.0	0.1	0.2	1.4	
Analysis of the tephra layer (119–122 cm) in the core SO202-27-6											
JR-2	76.8	0.06	12.9	0.58	0.09	0.50	0.01	3.88	5.24	97.4	5
	0.3	0.0	0.2	0.0	0.0	0.0	0.0	0.1	0.1	0.6	
last analyses											
AT	77.7	0.13	12.5	1.24	0.04	1.08	0.12	3.64	3.51	94.6	10
	0.2	0.0	0.1	0.1	0.0	0.0	0.0	0.1	0.2	0.9	
RIS1	76.8	0.07	13.0	0.68	0.13	0.47	0.01	4.01	4.88	97.5	10
	0.2	0.0	0.1	0.1	0.0	0.0	0.0	0.1	0.1	0.5	
JR-2 reference data (Imai et al., 1995, Geostandards Newsletter)											
	SiO_2	TiO_2	Al_2O_3	FeO*	MnO	CaO	MgO	Na_2O	K_2O	H_2O	
	75.69	0.07	12.72	0.77	0.112	0.5	0.04	3.99	4.45	1.41	

Note: AT tephra (Machida and Arai, 1976) was collected at Chigaki, Tateyama. RIS1 is obsidian collected at Wada Touge and using one of the house standards at Rissho University. JR-2 is obsidian collected at Wada Touge, held at the National Science Museum, Japan. JR-2 is the one of the Geological Survey of Japan (GSJ) geochemical reference samples (Imai *et al.*, 1995). The analytical order was RIS1, AT tephra, study samples, JR-2, AT tephra and RIS1. RIS1 and AT were used to monitor consistency in a series of analyses. JR-2 was analysed for comparison with other laboratories.